Characterization of a polarization-resolved high spectral resolution UV-visible spectrometer

J. Kim[1] and D. Kim[2,a)]
[1]*Korea Electrotechnology Research Institute, 28-1, Sungju-dong, Changwon, Kyungnam 641-120, Republic of Korea*
[2]*Department of Physics, Pohang University of Science and Technology, San 31, Hyojadong, Namgu, Pohang, Kyungbuk 790-784, Republic of Korea*

(Received 5 December 2007; accepted 18 February 2008; published online 24 March 2008)

To measure the degree of polarization of a plasma emission, a polarization-resolved UV-visible Czerny–Turner-type spectrometer was designed and constructed. For a high spectral resolution, $F=1$ m mirrors were used as a focusing and collimating mirrors and the incidence angles to the mirrors were determined to eliminate coma. The effect of astigmatism was reduced by designing the incidence angles to the mirrors to be as small as possible. The flat focal plane condition proposed by Reader [J. Opt. Soc. Am. **59**, 1189 (1969)] was used to determine the grating position. The measured spatial resolution was 170 μm. To simultaneously measure the intensities with two perpendicular polarizations, a calcite crystal was placed after the entrance slit of the spectrometer. The change in the imaging property of the spectrometer due to the calcite crystal was measured and minimized. The spectral resolution was experimentally measured with a laser produced plasma to be 0.05 nm at 348 nm. The resolving power measured is 6600. © *2008 American Institute of Physics.*
[DOI: 10.1063/1.2898704]

I. INTRODUCTION

A polarization-resolved (PR) spectrum can give us more information about a plasma than an intensity spectrum. Such PR spectra can be used to measure the degree of polarization of emission lines from plasmas and to measure the strength of a spontaneous magnetic field in laser produced plasmas. The degree of polarization of an emission line from plasma can be measured by a spectrometer equipped with a polarization resolving optics. The anisotropy of electron energy distribution of a plasma can be studied by measuring the degree of polarization of an emission line, which is one of the important topics in plasma polarization spectroscopy.[1] Plasma polarization spectroscopy has already been applied to various plasmas such as solar flares,[2] laser produced plasmas,[3,4] and tokamak plasmas.[5] The existence and the strength of a spontaneous magnetic field can be estimated by measuring the Zeeman splitting of the spectral lines in a laser produced plasma.[6] For both cases, a high spectral resolution PR spectrometer is needed to measure the intensities of different Zeeman multiplets.

A PR high spectral resolution spectrometer is a demanding tool for plasma spectroscopy. The PR spectrometer consists of two parts: one is a polarization resolving optic and the other a spectrometer. Typically, a plastic polarizer was placed in front of a spectrometer. However, in such a case, two different spectra, one for each polarization, are needed. To minimize the effect due to the intensity variation between two experiments, intensities for different polarizations must be simultaneously measured. For this purpose, we designed and constructed a PR Czerny–Turner-type spectrometer (CTS) with a calcite crystal as a polarizer. The aberration in the CTS which uses off-axis mirrors must be reduced to get a high spectral resolution. The imaging and spectral properties of the spectrometer were investigated.

II. DESIGN OF CTS

A CTS consists of an entrance slit, a collimating mirror, a plane grating, a focusing mirror, and a detector, as in Fig. 1. The collimating and focusing mirrors in the spectrometer make an image of the entrance slit on the detector. Due to the aberration from the mirrors, the spectral line broadens. A double mirror system is more flexible compared to a single mirror system. If the incidence angle to the curved mirror is properly chosen, the coma-type aberration can be eliminated at one wavelength. The grating position can be designed to get a flat focal plane.[7] The design goal of the spectrometer was to get a high spectral resolution and to minimize the effect of astigmatism to enhance imaging property in the lateral direction (corresponding to the direction perpendicular to the dispersion direction). To get a high spectral resolution, long focal-length spherical mirrors were used for the collimating and focusing mirrors. The incidence angles to the collimating and focusing mirrors were chosen to reduce coma at 300 nm. The coma correction condition is

$$\frac{\sin\beta}{\sin\alpha}=\frac{R_f^2}{R_c^2}\frac{\cos^3\beta}{\cos^3\alpha}\frac{\cos^3\alpha_g}{\cos^3\beta_g}, \tag{1}$$

where α and β are the incidence angles to the collimating and focusing mirrors, α_g and β_g are the incidence angles to and diffraction angle from the grating, and R_f and R_c are the radii of curvature of the focusing and collimating mirrors, respectively. The astigmatism blurs the vertical image of the slit on the detector. To minimize this effect, the incidence angles to each mirror were designed to be near

a)Electronic mail: kimd@postech.ac.kr. FAX: +82-54-279-5564.

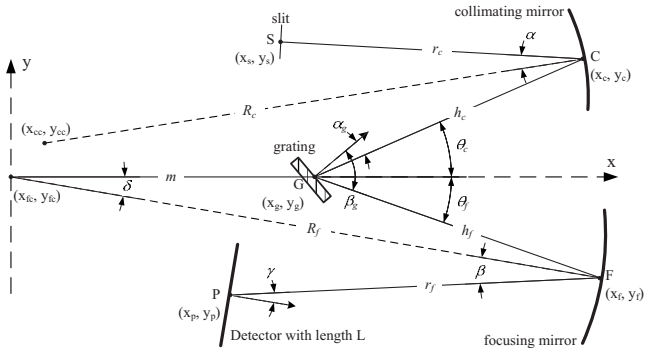

FIG. 1. Schematic diagram of a CTS. S, C, G, F, and P denote the center of slit, collimating mirror, grating, focusing mirror, and detector, respectively. R_c and R_f are the radii of curvature of collimating and focusing mirrors, respectively. Dashed line indicates the normals of the mirrors.

normal. Under these two conditions, the incidence angle was chosen.

The focal plane can be adjusted by changing the grating position m. The position of the focal plane can be calculated by

$$\frac{x}{R_f} = \frac{1}{2} - \frac{1}{4}\left[1 - 3\left(\frac{m}{R_f}\right)^2\right]\theta_f^2 + \frac{1}{48}\left[1 - 30\left(\frac{m}{R_f}\right)^2 + 48\left(\frac{m}{R_f}\right)^3 - 27\left(\frac{m}{R_f}\right)^4\right]\theta_f^4,$$

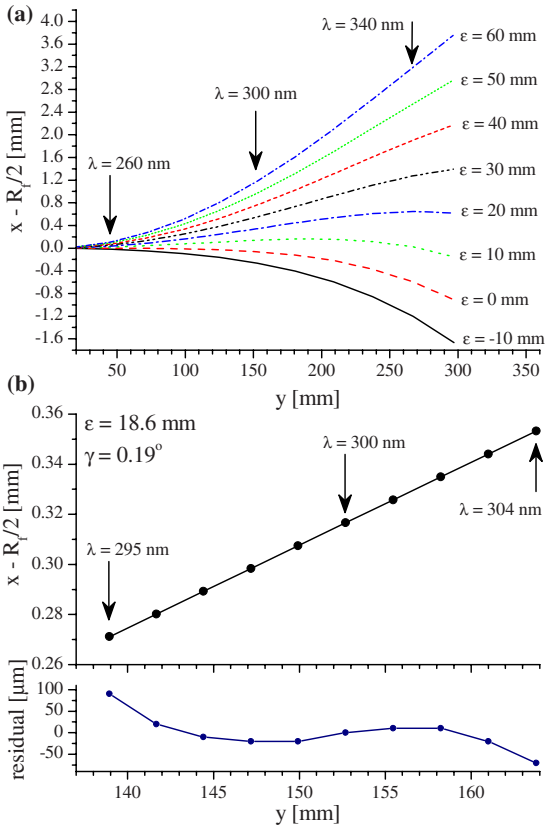

FIG. 2. (Color online) Focal plane position. ε is the correction factor of the grating position. (a) The focal plane in a wide spectral range with different ε. (b) The focal plane with flat condition. In (b), dots are the calculated focal position with different wavelengths. The solid line is the linear fit of the focal positions.

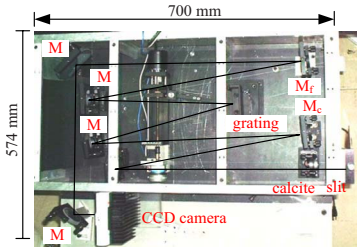

FIG. 3. (Color online) A picture of the spectrometer. M_c is the collimating mirror and M_f is the focusing mirror. Flat mirrors are used as folding mirrors to reduce the size of the spectrometer indicated M.

$$\frac{y}{R_f} = \frac{1}{2}\theta_f + \left[-\frac{1}{12} + \frac{3}{4}\left(\frac{m}{R_f}\right)^2 - \left(\frac{m}{R_f}\right)^3\right]\theta_f^3, \quad (2)$$

where m is the grating position and θ_f is the diffraction angle measured from the x axis. Figure 2 shows the focal plane positions, where $\varepsilon = m - R_f/\sqrt{3}$ is the grating position correction factor. Figure 2(a) shows the optimal focal plane position in a wide spectral range with different ε. To make a flat focal plane, the deviation of focal points from a straight line must be minimized in the whole spectral range. This can be achieved by minimizing the deviation of Δ in the spectral range. Δ is given as

$$\Delta = \frac{y(\varepsilon,\lambda) - y(\varepsilon,\lambda_c)}{x(\varepsilon,\lambda) - x(\varepsilon,\lambda_c)}, \quad (3)$$

where λ_c is the center wavelength. Figure 2(b) shows the minimum deviation curve corresponding to the flat focal plane condition. In this case, for a computed ε equal to 18.6 mm, it is necessary to use a 25 mm side detector to cover the 295–304 nm spectral range. The flat focal plane is not parallel to the y axis but inclined at an angle of 0.19°. The focal plane deviation due to this angle is only 80 μm. In the alignment of the spectrometer, the detector was set parallel to the y axis. Figure 3 shows the picture of the spectrometer. Flat folding mirrors are used to reduce the size of the spectrometer. A calcite crystal was employed to resolve polarization (as described in Sec. III).

The minimum incidence angles to the mirrors are limited by the size of the optics. The image along the lateral direction is blurred by the oblique incidence angle of the mirrors, i.e., astigmatism. The spatial resolution was measured with a

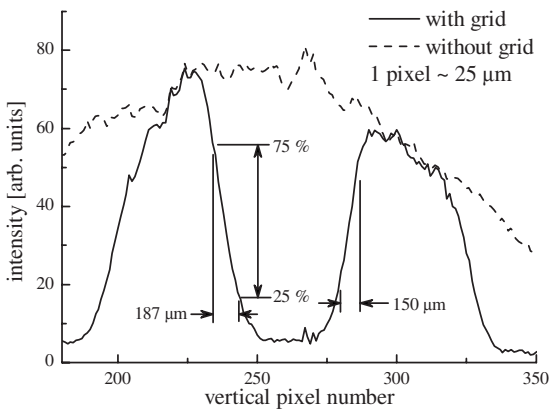

FIG. 4. Measurement of the spatial resolution using a grid at the entrance slit position. The slit was illuminated by a standard lamp.

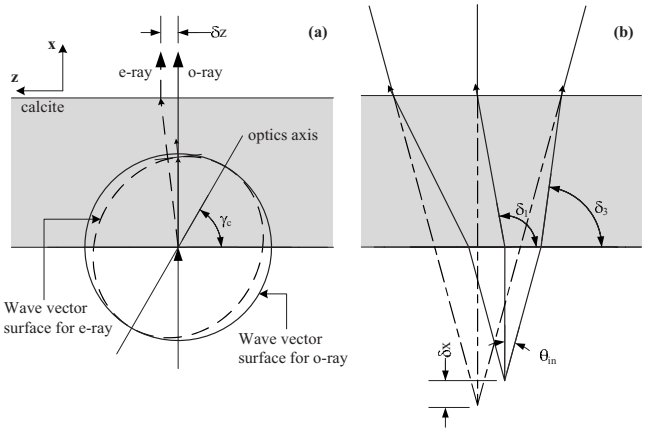

FIG. 5. Ray displacement by a calcite crystal. (a) The displacement of *e* ray. (b) The source displacement.

standard lamp and a 1 mm wide, 1 mm separated grid as a fiducial. The grid was placed at the entrance slit. Figure 4 shows the cross section of the image of the grid in the lateral direction. The measured spatial resolution in the lateral direction is 170 μm.

III. THE EFFECT OF CALCITE CRYSTAL

To separate two polarizations, a calcite crystal was placed just after the entrance slit. The birefringent property of a properly cut calcite crystal, which is a negative uniaxial crystal, separates two perpendicular polarizations, as shown in Fig. 5(a). One of the beams whose polarization is perpendicular to the principal section (the plane contains the optic axis of the crystal and the incidence axis) is called an ordinary ray, *o* ray. The other beam whose polarization is parallel to the principal section is called an extraordinary ray, *e* ray. The ray direction of *e* ray is normal to the wave vector surface, as in Fig. 5(a). The beam displacement of *e* ray can be calculated by

$$\delta z = t\frac{(n_o^2 - n_e^2)\tan\gamma}{n_o^2 + n_e^2\tan\gamma}, \tag{4}$$

where n_o and n_e are the indices of refraction for *o* ray and *e* ray, respectively, γ_c is the angle between the crystal boundary plane and the optic axis, and t is the thickness of the crystal. The index of refraction can be found in Ref. 8. The calcite crystal with $\gamma_c = 50°$ was used to maximize the separation between the *e* ray and *o* ray. As shown in Fig. 6, after the calcite crystal, the beam is vertically split, forming two layers of spectrum: the upper layer is the spectrum for *e* ray and the lower for *o* ray.

The refraction of the calcite crystal displaces the source along the *x* direction, as shown in Fig. 5(b). The amount of the displacement is different for different polarizations. The spectral line is broadened due to this displacement. The detector position was changed to reduce the broadening due to this effect.

The displacement of the source for different polarizations can be estimated by Huygens principle, as in Fig. 5(b). For *o* ray, the displacement δx can be calculated by

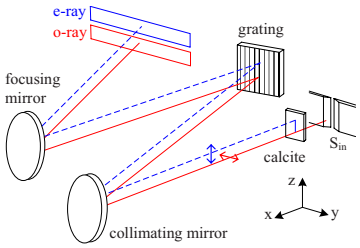

FIG. 6. (Color online) Schematic diagram of the spectrometer with a calcite crystal. The solid line shows the light path for *o* ray whose polarization is horizontal. The dashed line shows the path for *e* ray whose polarization is vertical.

$$\delta x \cong t\left(1 - \frac{n_i}{n_o}\right), \tag{5}$$

where n_i is the index of refraction of the incidence medium and t is the thickness of the crystal. The displacement for *e* ray is given as

$$\delta x = t\left[1 + \frac{1}{\tan\theta_{\text{in}}}\left(\frac{1}{\tan\delta_3} - \frac{1}{\tan\delta_1}\right)\right], \tag{6}$$

where θ_{in} is the half of the beam divergence, and δ_1 and δ_3 are the refraction angles measured from the boundary of the crystal and can be calculated as

$$\tan\delta = \frac{n_o^2 + n_e^2\tan(\gamma - \theta_{\text{out}})\tan\gamma}{n_e^2\tan(\gamma - \theta_{\text{out}}) - n_o^2\tan\gamma}, \tag{7}$$

where θ_{out} is the refraction angle of *e* ray and can be calculated by

$$\sin\theta_{\text{out}} = \left[1 + \left(\frac{n_o^2}{n_e^2} - 1\right)\sin^2\alpha\right]^{1/2}\sin\theta_{\text{in}},$$

$$\alpha = \frac{\pi}{2} - \gamma + \theta_{\text{out}}. \tag{8}$$

Figure 7 is the displacements of the source for different wavelengths with an optic axis angle of 50°. The displacements of the slit image is −9% of the thickness of the calcite for *e* ray at 300 nm and +42% for *o* ray. The plus sign means that the slit position moves closer to the collimating mirror.

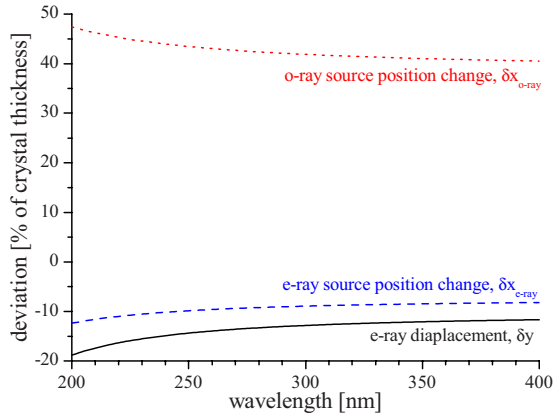

FIG. 7. (Color online) Displacement of the source for different wavelengths at an optics axis of 50°.

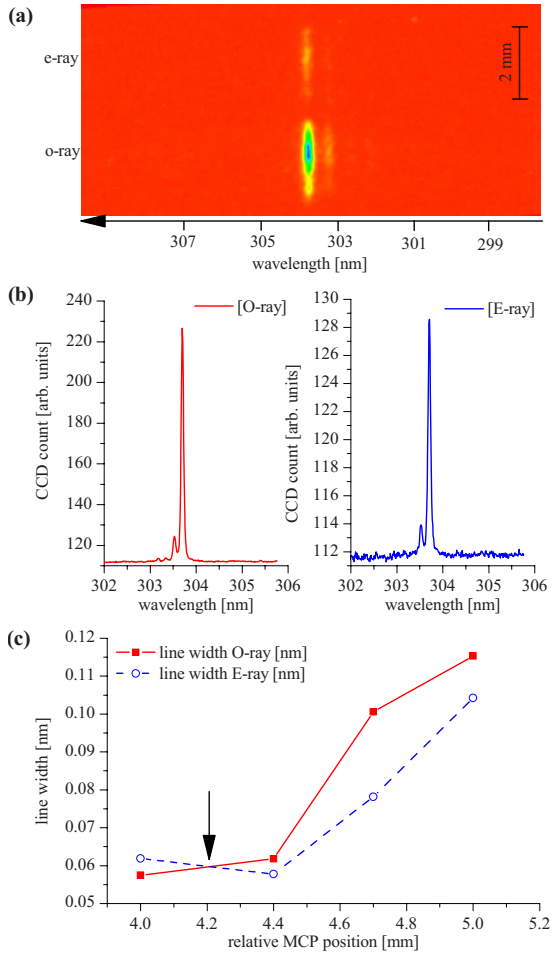

FIG. 8. (Color online) Measured spectrum with Hg standard lamp. (a) The measured spectrum. (b) The cross section of the spectrum. (c) The change of the spectral width of Hg 303.7 nm line for different detector positions.

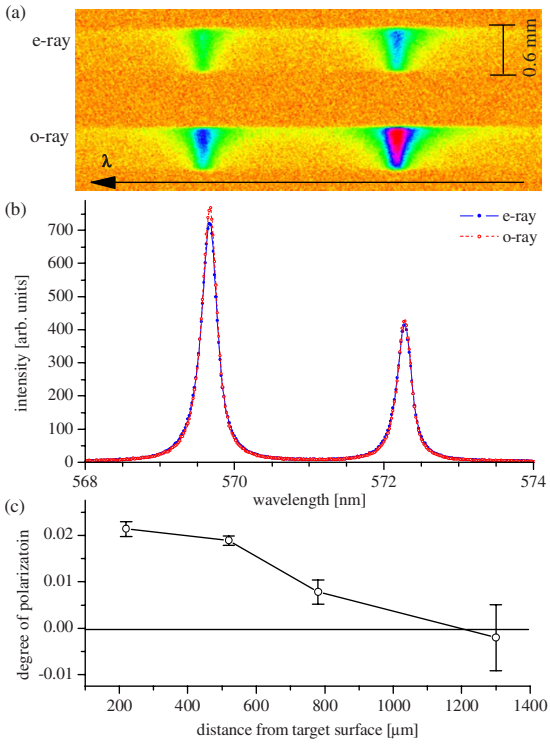

FIG. 9. (Color online) PR spectra. (a) PR spectral image on the focal plane. (b) The cross section of (a) at 200 μm from the target surface. The open circle is *o* ray spectrum and the closed circle is *e* ray. (c) The measured degree of polarization at different distances from the target surface.

To reduce the difference in the spectral line broadening by the calcite crystal between *e* ray and *o* ray, the detector position needed to be adjusted.

The spectral line broadening due to the source displacement was measured using a standard lamp. Figure 8 shows the measured spectrum and linewidths for different detector positions. A charge coupled device (CCD) camera (Photometrics SenSys) was used as a detector. The pixel size of the CCD camera was 13 μm and the total number of pixels was 768×512. The slit width was 50 μm. The pixel positions were converted to wavelength using a linear fit to known Hg spectral lines. This calibration yielded that 100 pixels corresponding to 1 nm separation in wavelength. To remove the overlapping of two spectra, the slit height of 2 mm was used. In Fig. 8(a), the spectra with different polarizations were well separated. The intensity difference between *e* ray and *o* ray is due to the different efficiencies of the grating for the different polarizations. Figure 8(b) shows the cross section of the spectrum Fig. 8(a). Note that the linewidth is different between *e* ray and *o* ray as expected. Figure 8(c) shows the spectral width of *e* ray and *o* ray for different detector positions. The position for the minimum spectral linewidth is different for *e* ray and *o* ray due to the different source displacements. The vertical arrow indicates the detector position where the spectral widths of *e* ray and *o* ray become equal. The detector was set at this position.

IV. PLASMA SPECTRA MEASUREMENT

To characterize the performance of the spectrometer, a laser produced plasma was used. A Nd/Glass laser was used to generate laser produced plasmas. The laser energy was 6 mJ and the pulse duration was 3 ns. A CCD camera was used as a detector.

Figure 9(a) shows the PR spectra from Al III ion. The upper layer is *e* ray spectrum and the lower is *o* ray. The polarization direction of *e* ray is parallel to the laser incidence direction due to the target and relay optics geometry.

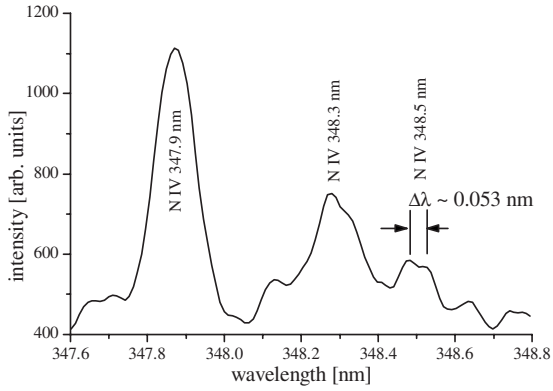

FIG. 10. Measurement of spectral resolution.

TABLE I. Design parameter of 1 m CTS.

Parameter	Meaning	Value
r_c	Distance between slit and collimating mirror	998.09 mm
α	Incidence angle to collimating mirror	3.54°
R_c	Radius of curvature of collimating mirror	2000 mm
h_c	Distance between collimating mirror and grating	854.24 mm
α_g	Incidence angle to grating	12.6°
m_g	Diffraction order	−1
σ	Number of groove	2400 lines/mm
λ_c	Center wavelength	300 nm
β_g	Diffraction angle	30.13°
h_f	Distance between grating and focusing mirror	851.05 mm
β	Incidence angle to focusing mirror	5.06°
R_f	Radius of curvature of focusing mirror	2000 mm
r_f	Distance between focusing mirror and detector	996.1 mm

The polarization direction of *o* ray is parallel to the target surface. Figure 9(b) is the cross section of the spectrum.

Due to the spatial resolving property of the spectrometer, the space-resolved polarization measurement is possible. Figure 9(b) is the spectrum at 200 μm from target surface. Figure 9(c) shows the measured degree of polarization for different distance from target surface. Due to the symmetry, the transition from $J=1/2$ to $J=1/2$ cannot be polarized. The intensity difference in *e* ray and *o* ray for Al III 572.27 nm line is due to the different sensitivities of the spectrometer for different polarizations. This transition line was used to correct the different efficiencies of the grating for different polarizations.[4] In Fig. 9(b), the intensity was corrected using $J=1/2$ to $J=1/2$ transition. The degree of polarization is defined as

$$P=\frac{I_{\parallel}-I_{\perp}}{I_{\parallel}+I_{\perp}}=\frac{I_{e\ \mathrm{ray}}-I_{o\ \mathrm{ray}}}{I_{e\ \mathrm{ray}}+I_{o\ \mathrm{ray}}}, \tag{9}$$

where $I_{\parallel}$ and $I_{\perp}$ denote the light with polarization parallel and perpendicular to the laser incidence axis, respectively. The measured degree of polarization for Al III $4s^2S_{1/2}$-$4p^2P^o_{3/2}$, 569.66 nm was 2% (with an error bar of 0.2%) at 200 μm from the target surface. However, at 1 mm from the target surface, the emission light was not polarized. This demonstrates that this spectrometer can resolve the degree of polarization with an accuracy of 0.2%.

A nitrogen plasma was used to measure the spectral resolution of the spectrometer. In this case, a frequency-doubled Nd/YAG (yttrium aluminum garnet) laser was used to generate laser produced plasmas. The laser energy was 300 mJ and the pulse duration was 7 ns. The imaging intensifier which consists of microchannel plate (MCP) and phosphor screen was used. A 7 ns high-voltage pulse was applied to MCP for time-resolved measurement. Figure 10 shows the *e* ray spectrum from the nitrogen plasma. The $2s3s^3S$-$2s3p^3P_o$ transition line is split due to the spontaneous magnetic field very close to the target surface. The resolved line separation is 0.05 nm at 348.5 nm, which yields the resolving power ($R_p \equiv \lambda/\Delta\lambda$) of 6600.

V. CONCLUSIONS

For a high spectral resolution, a coma-corrected CTS with $F=1$ m was designed and constructed. The design parameters of the spectrometer's components are given in Table I. To record the magnitude of the two perpendicular polarizations at the same time, a calcite crystal was used after the entrance slit of the spectrometer. For the largest separation of the two spectra of two different polarizations in the direction perpendicular to the beam propagation, the optic axis of the crystal was set at an angle of 40 °(90 °$-\gamma_c$) with respect to the beam direction.

The imaging property and the spectral resolution were experimentally measured with a plasma as a source. The spatial resolution of the spectrometer was measured to be 170 μm and the spectral resolving power to be higher than 6600 at 348 nm. This spectrometer can resolve the degree of polarization with an accuracy of 0.2%.

This PR spectrometer is a proper tool to measure the degree of polarization of the emission lines from laser produced plasmas because the intensity of the different polarization light can be simultaneously measured. This is important for the single shot experiment to eliminate the effect of the shot to shot variation of the plasma. Due to the high spectral resolution of the spectrometer, this spectrometer is a good tool to measure a spontaneous magnetic field by the Zeeman splitting spectra.

ACKNOWLEDGMENTS

This work has been supported by BK21 project funded by the Korea Research Foundation.

[1] T. Fujimoto and S. A. Kazantsev, Plasma Phys. Controlled Fusion **39**, 1267 (1997).
[2] E. Haug, Sol. Phys. **71**, 77 (1981).
[3] J. C. Kieffer, J. P. Matte, H. Pepin, M. Chaker, Y. Beaudoin, T. W. Johnston, C. Y. Chen, S. Coe, G. Mourou, and J. Dubau, Phys. Rev. Lett. **68**, 480 (1992).
[4] J. Kim and D. Kim, Phys. Rev. E **66**, 017401 (2002).
[5] T. Fujimoto, H. Sahara, T. Kawachi, T. Kallstenius, M. Goto, H. Kawase, T. Furukubo, T. Maekawa, and Y. Terumichi, Phys. Rev. E **54**, R2240 (1996).
[6] E. A. McLean, J. A. Stamper, C. K. Manka, H. R. Griem, D. W. Droemer, and B. H. Ripin, Phys. Fluids **27**, 1327 (1984).
[7] J. Reader, J. Opt. Soc. Am. **59**, 1189 (1969).
[8] G. Ghosh, Opt. Commun. **163**, 95 (1999).